catalysts

Article

Effects of Coordination Ability of Nitrogen-Containing Carboxylic Acid Ligands on Nieuwland Catalyst

Yanhe You [1], Juan Luo [1], Jianwei Xie [1,2,*], Jinli Zhang [3] and Bin Dai [1,*]

1 School of Chemistry and Chemical Engineering/Key Laboratory for Green Processing of Chemical Engineering of Xinjiang Bingtuan, Shihezi University, North 4th road, Shihezi 832003, China; shzu_yanheyou@sina.com (Y.Y.); shzu_juanluo@sina.com (J.L.)
2 Industrial Technology Research Institute, Xinjiang Production and Construction Corps, Shihezi 832003, China
3 School of Chemical Engineering and Technology, Tianjin University, Tianjin 300072, China; zhangjinli@tju.edu.cn
* Correspondence: cesxjw@foxmail.com (J.X.); db_tea@shzu.edu.cn (B.D.); Tel.: +86-993-205-7213 (J.X. & B.D.); Fax: +86-993-205-7270 (J.X. & B.D.)

Received: 21 July 2018; Accepted: 13 August 2018; Published: 17 August 2018

Abstract: This article investigated the effect of three nitrogen-containing carboxylic acid ligands for the Nieuwland catalyst system. The catalyst system containing 4.5% *N*-(2-acetamido) iminodiacetic acid exhibited improved catalytic activity with excellent performance. The yield of monovinylacetylene (MVA) was maintained at 36.7% after 24 h, which was increased by 17.1% relative to the Nieuwland catalyst system. Based on a variety of analyses on the crystals precipitated from the catalyst solutions, it can be inferred that the outstanding performance and lifetime of the catalysts were related to the abilities of these ligands to form strong coordination with Cu^+ ions and stabilize them.

Keywords: Nieuwland catalyst; acetylene dimerization; monovinylacetylene; nitrogen-containing carboxylic acid ligands

1. Introduction

The dimerization of C_2H_2 to produce monovinylacetylene (MVA) is the key step for the C_2H_2-based process in the synthesis of chloroprene rubber (CR) (Scheme 1), which is widely used in the adhesive and automobile industries [1,2]. The traditional catalyst for C_2H_2 dimerization is the Nieuwland catalyst, which is comprised of CuCl, HCl and NH_4Cl (or KCl) in an aqueous media [3–5]. Despite the long history and practical application of the Nieuwland catalyst [6–8], drawbacks, such as low C_2H_2 conversion rate and low MVA selectivity, still exist.

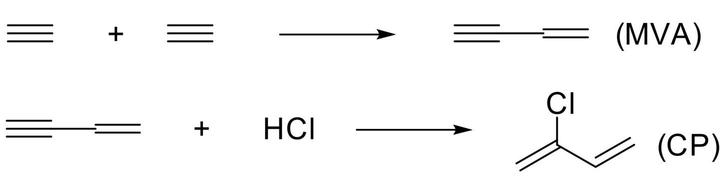

Scheme 1. C_2H_2-based process for 2-chloro-1,3-butadiene (CP) production.

Recently, some of these drawbacks have been overcome by the addition of a second metal or ligand/additive to the Nieuwland catalytic system, which can enhance the activity or the lifetime of the catalyst. For example, the addition of a certain amount of urea [9], phosphine ligands [10], $LaCl_3$ [11,12], $CeCl_3$ [13] or D/L-alanine [14] to the Nieuwland catalyst can improve the C_2H_2 conversion and/or MVA selectivity. We have also found that $SrCl_2$ [15], $ZnCl_2$ [16], and PEGs [17]-modified Nieuwland catalysts can increase the selectivity of MVA while extending the lifetime of the catalyst. In fact, the $Cu_nCl^-_{n+1}$ $(nCuCl + Cl^- \rightarrow Cu_nCl^-_{n+1})$ formed via the combination of CuCl and the solubilizer in the catalyst solution actually contributes to this reaction. The electron transfer from Cu in $Cu_nCl^-_{n+1}$ to the π^* orbital of the C≡C bond is a critical process in the C_2H_2 dimerization reaction, which acts as an activating C≡C bond [18]. Hence, the electron cloud density of Cu (I) in $Cu_nCl^-_{n+1}$ determines the activity of the Nieuwland catalytic system. In 2017, we found that iminodiacetic acid [19] used as a ligand to modify the Nieuwland catalyst can simultaneously increase C_2H_2 conversion rate and MVA selectivity, and extend the lifetime of the catalyst. As part of our continuing work, we have observed the C_2H_2 dimerization reactions catalyzed by the Nieuwland catalysts that were modified by nitrilotriacetic acid, *N*-(2-hydroxyethyl)iminodiacetic acid, and *N*-(2-acetamido) iminodiacetic acid (ADA). The three kinds of ligand-modified Nieuwland catalysts can improve the C_2H_2 conversion rate. In particular, using the ADA-modified Nieuwland catalyst, 46.7% C_2H_2 conversion and 78.1% MVA selectivity were achieved, and the yield of MVA increased by 17.1% compared with the conventional Nieuwland catalyst. Ligand coordination ability, structures, and reaction mechanisms of these catalysts are also discussed.

2. Results and Discussions

2.1. Catalytic Activities of NC and N-NC

Initially, the activities of NC, **N$_1$**-NC, **N$_2$**-NC, and **N$_3$**-NC were tested under the same reaction conditions (the reaction temperature was 80 °C and the space velocity of C_2H_2 was 105 h^{-1}). Figure 1 and Table 1 show the data obtained from the experiment. The data suggests the Nieuwland catalyst containing three ligands can increase the conversion rate of C_2H_2. The sequence of catalyst activity was **N$_3$**-NC > **N$_2$**-NC > **N$_1$**-NC > NC. Among them, **N$_3$**-NC showed the best catalytic performance in this reaction with 46.7% C_2H_2 conversion. For MVA selectivity, all the **N**-NCs demonstrated good selectivity in a range of 78–80% and these ligands improved the selectivity of MVA in varied degrees compared with the NC. As shown in Figure 2 and Table 2, we performed the 24 h lifetime tests and **N$_3$**-NC exhibited high catalytic activity and stability. The C_2H_2 conversion and MVA selectivity did not decrease greatly within 24 h as shown in Figure 2. By contrast, NC and HCl-NC exhibited distinctly lower catalytic performance and stability.

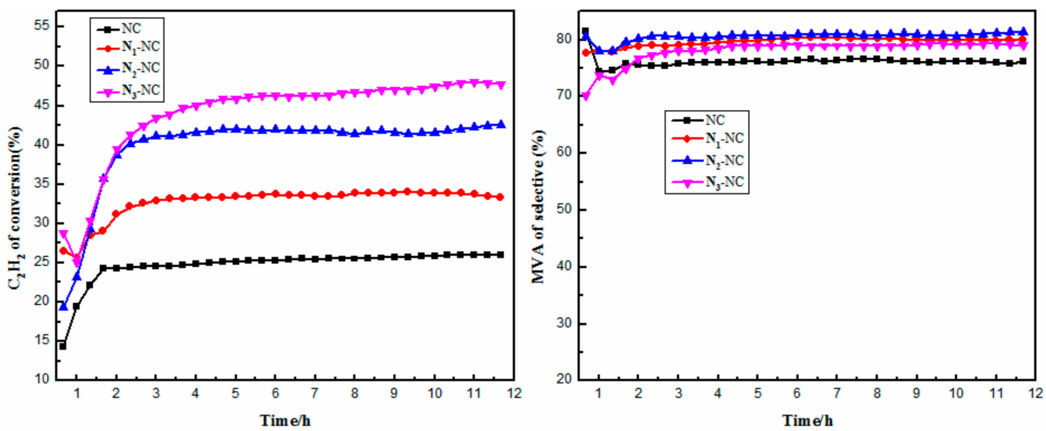

Figure 1. Catalytic performances testing for NC and **N**-NC in C_2H_2 dimerization reaction.

Table 1. Effect of NC and **N**-NC on acetylene conversion and MVA selectivity in acetylene dimerization.

Catalysts	C_2H_2 Conversion (%)	MVA Selectivity (%)	Yield (%)
NC	25.5	76.1	19.4
$\mathbf{N_1}$-NC	33.6	79.6	26.7
$\mathbf{N_2}$-NC	41.6	80.6	33.5
$\mathbf{N_3}$-NC	46.7	78.1	36.5

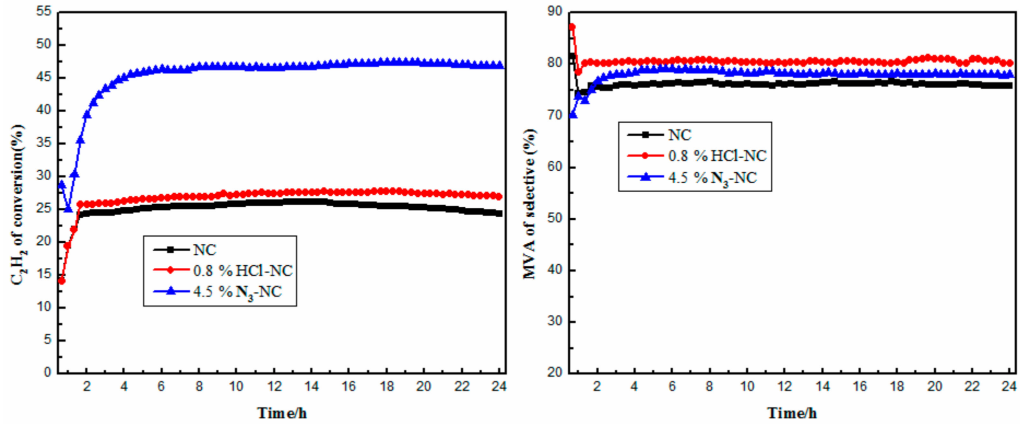

Figure 2. Lifetime testing of NC, 4.5% $\mathbf{N_3}$-NC and 0.8% HCl-NC.

Table 2. Effect of NC, 4.5% $\mathbf{N_3}$-NC and 0.8% HCl-NC on acetylene conversion and MVA selectivity in acetylene dimerization.

Catalysts	C_2H_2 Conversion (%)	MVA Selectivity (%)	Yield (%)
NC	25.5	76.1	19.4
0.8% HCl-NC	27.2	80.5	21.9
4.5% $\mathbf{N_3}$-NC	46.9	78.3	36.7

2.2. Compositions of the Crystals

Considering the influence of the coordination ability of $\mathbf{N_1}$, $\mathbf{N_2}$, and $\mathbf{N_3}$ on the activity of the Nieuwland catalyst, we used the following characterization methods to investigate the structures of NC, $\mathbf{N_1}$-NC, $\mathbf{N_2}$-NC, and $\mathbf{N_3}$-NC, and the coordination ability of these ligands.

The FT-IR spectrums of three ligands and four crystals were shown in Figure 3. The peaks at 3440 and 3160 cm^{-1} are the characteristic peaks of N–H [7] and O–H respectively. In the catalyst solution, NH_4^+ was hydrolyzed to produce NH_3 ($NH_4^+ + 2H_2O = NH_3 \cdot H_2O + H_3^+O$) [7]; thus, we inferred that the crystals contained H_2O and NH_3. As shown in Figure 3b, the peak at 1718 cm^{-1} is assigned to the characteristic peaks of C=O in the carboxyl group. Nevertheless, compared with $\mathbf{N_1}$, the C=O stretching peak, which was red, shifted by nearly 95 cm^{-1}, which was mainly due to the formation of complexes between the carboxyl groups that lost their protons to the ligands and copper ions. Similarly, the characteristic peaks of C=O in crystals C and D, which were red, shifted by 85 and 56 cm^{-1}, respectively. The N–H vibration absorption peak of the amide group, which was red and presented at 1675 cm^{-1} as shown in Figure 3d, shifted by 84 cm^{-1}. The IR spectra of the crystals show that there was coordination between the three ligands and copper ions, as anticipated.

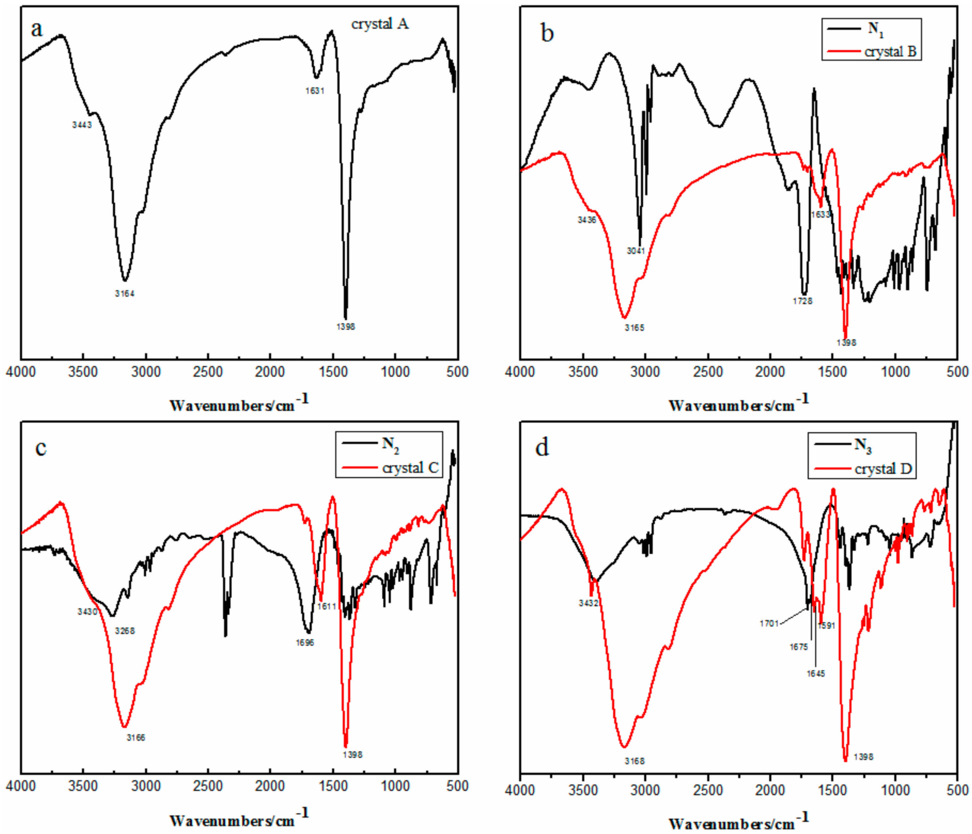

Figure 3. FT-IR spectra of the $\mathbf{N_1}$, $\mathbf{N_2}$, $\mathbf{N_3}$ and crystal A-D. (**a**) crystal A; (**b**) $\mathbf{N_1}$ and crystal B; (**c**) $\mathbf{N_2}$ and crystal C; (**d**) $\mathbf{N_3}$ and crystal D.

In order to further determine the ligand coordination ability, we performed TG analysis on the crystals (Figure 4). As shown in Figure 4, the initial weight loss of these crystals started at 100 °C because of the loss of crystal water. Obviously, the second weight loss of these crystals was because of the loss of NH_3, which is demonstrated by TPD-MS (Figure 5). XRD studied the residue after calcination of these crystals at 450 °C and found that it contained CuCl and $CuCl_2$ (Figure 6). However, compared with crystal A, crystals B, C, and D suffered weight loss at 365.9, 365.1, and 370 °C, respectively. This phenomenon showed that there was the coordination between these three ligands and copper elements, requiring high temperature desorption. Therefore, the order of these ligands' coordination ability is likely to be $\mathbf{N_3} > \mathbf{N_2} \approx \mathbf{N_1}$. XRF examination of the crystals showed that their Cu/Cl atomic ratios were 2:3. Consequently, we can infer from the data in Table 3 that the compositions of crystals A-D are $Cu_2Cl_3 \cdot 6NH_3 \cdot (1/20)H_2O$, $Cu_2Cl_3 \cdot (1/9)C_6H_9NO_6 \cdot 8NH_3 \cdot (2/3)H_2O$, $Cu_2Cl_3 \cdot (1/7)C_6H_{11}NO_5 \cdot (17/2)NH_3 \cdot (1/2)H_2O$, and $Cu_2Cl_3 \cdot (1/9)C_6H_{10}N_2O_5 \cdot 8NH_3 \cdot (1/2)H_2O$, respectively.

Table 3. The crystals weight loss data from TG/DTG.

Catalysts	The First (%)	The Second (%)	The Third (%)	The Fourth (%)
crystal A	0.28	30.04	0	69.68
crystal B	2.81	31.21	4.86	54.18
crystal C	1.89	31.72	6.44	52.13
crystal D	2.23	31.70	5.70	54.56

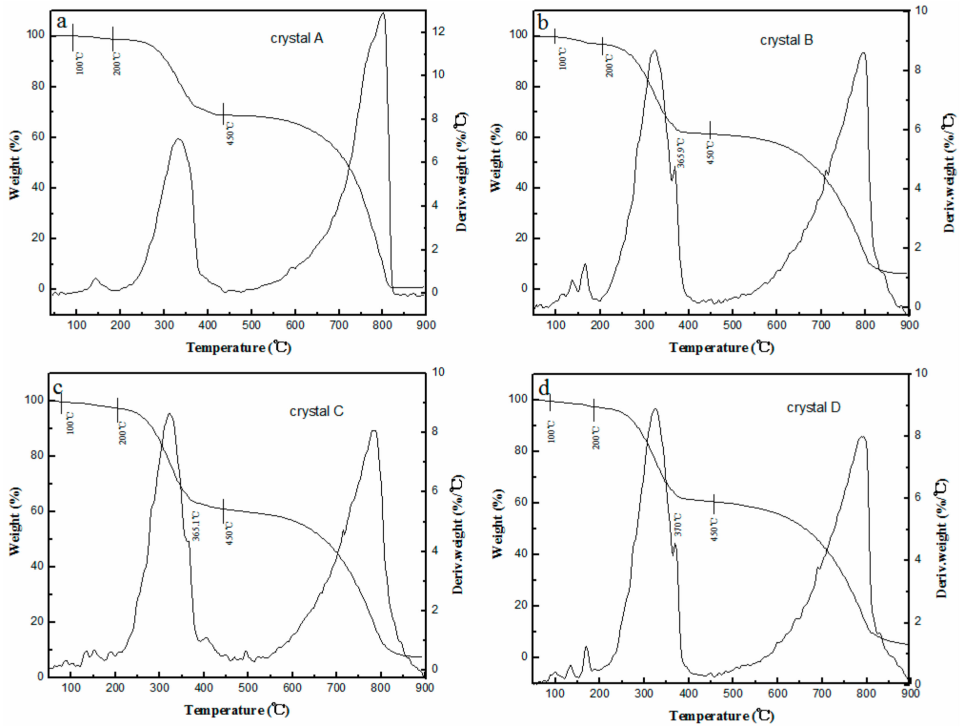

Figure 4. TG/DTG thermograms for the crystals. (**a**) crystal A; (**b**) crystal B; (**c**) crystal C; (**d**) crystal D.

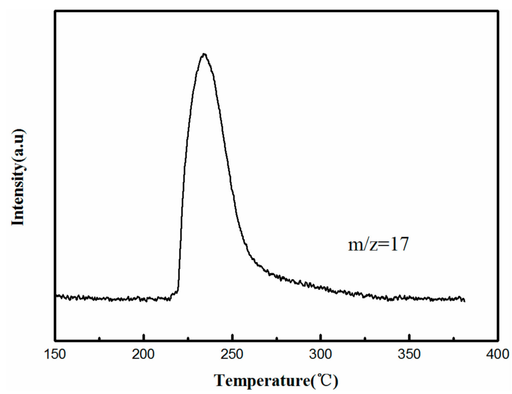

Figure 5. TPD-MS spectra of desorption of the crystals.

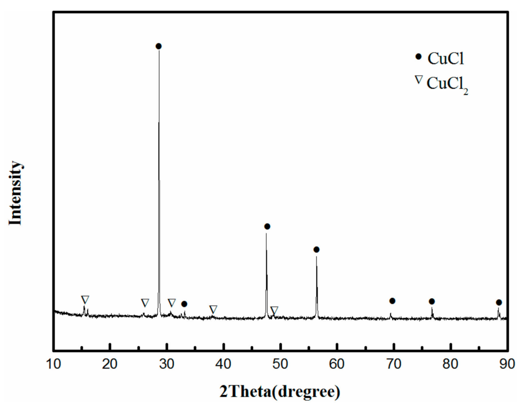

Figure 6. XRD study of heating product (450 °C) of the crystals.

2.3. The Ligands Coordination Ability Analysis

As shown in Figure 7, the XPS results showed that the binding energy of Cu $2p_{3/2}$ for crystals B, C, and D, respectively, exhibited the 0.23, 0.28, and 0.43 eV negative shifts, as compared with the crystal A. The transfer of electrons from the ligands to Cu^+ increases the electron cloud density of Cu^+, causing this negative shift. Among the three ligands, $\mathbf{N_1}$ and $\mathbf{N_2}$ had similar coordination ability; however, they were relatively weaker than $\mathbf{N_3}$. The TG analysis results of the crystals also prove this conclusion. The $\mathbf{N_3}$ in crystal D required a higher desorption temperature than $\mathbf{N_1}$ and $\mathbf{N_2}$ in crystals B and C, whereas $\mathbf{N_1}$ and $\mathbf{N_2}$ required similar desorption temperatures. The UV-Vis spectra of the crystals further confirmed these results (Figure 8). The band in the range 300–850 nm can be ascribed to the charge transfer from Cl^- to Cu (I) [17]. In crystal D, the blue shift of the absorption band of Cu (I) was approximately 50 nm as compared with that in crystal A, mainly because the increased electron density of Cu (I) made the transfer of electrons from Cl^- to Cu (I) more difficult and required higher energy. However, the absorption band of Cu (I) for crystals B and C was blue and shifted by ≈30 nm. The order of the ligands' coordination ability was further confirmed to be $\mathbf{N_3} > \mathbf{N_2} \approx \mathbf{N_1}$.

From what has been discussed above, a high electron density of Cu (I) helped to increase the activity of the catalyst in C_2H_2 dimerization. Therefore, as described in Figures 3 and 4, $\mathbf{N_3}$-NC showed the best catalytic performance and stability due to it having the most powerful electronic donation and coordination capacity of $\mathbf{N_3}$ with Cu (I) among the three tested ligands. However, $\mathbf{N_2}$-NC exhibited better catalytic performance than $\mathbf{N_1}$-NC, mainly because $\mathbf{N_1}$ had a greater acidity than $\mathbf{N_2}$ in the catalyst solution and therefore inhibited the activity of the catalyst. Thus, the suitable acidity and strong coordination ability of the ligands helped to improve the activity of the catalyst.

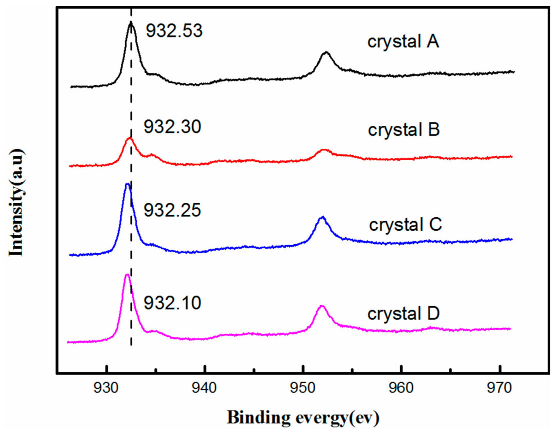

Figure 7. XPS spectra of the crystal A, crystal B, crystal C and crystal D for Cu 2p.

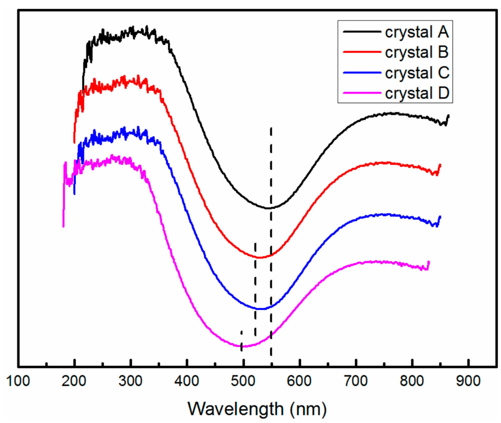

Figure 8. UV-Vis spectra of the crystal A, crystal B, crystal C and crystal D.

2.4. Correlation between the Amount of Copper (I) and Catalytic Activity

It is well known that Cu^+ is the main active component of the Nieuwland catalyst, and it has been reported in our previous work that the content of Cu^+ is related to the activity of the anhydrous Nieuwland catalyst [20]. Therefore, we investigated the valence charges of copper species using high-resolution XPS. The results are presented in Figure 9 and Table 4. The content of Cu^+ used in **N$_3$**-NC was higher than that used in other catalysts (Table 4), which further demonstrated the outstanding catalytic performance of **N$_3$**-NC (Figure 1). This phenomenon may be due to the fact that **N$_3$** can stabilize the Cu^+ content and inhibit the loss of Cu^+ content in the catalytic system. This observation can explain why **N$_3$**-NC possessed higher initial catalytic activity and longer service life than NC (Figure 2). In summary, the strong coordination ability of the ligand can be helpful to further improve the activity of the Nieuwland catalyst by stabilizing Cu (I).

Table 4. The relative contents and binding energies of copper species in fresh and used catalyst.

Catalysts	Area%, Binding Energy (eV)			
	Cu^+		Cu^{2+}	
	Fresh	Used	Fresh	Used
NC	85.38(932.54)	66.03(932.56)	14.62(934.90)	33.97(934.98)
N$_1$-NC	85.34(932.35)	73.05(932.31)	14.66(934.75)	26.95(934.69)
N$_2$-NC	85.97(932.22)	75.53(932.15)	14.03(934.61)	24.47(934.58)
N$_3$-NC	85.94(932.10)	80.14(932.01)	14.06(934.50)	19.86(934.50)

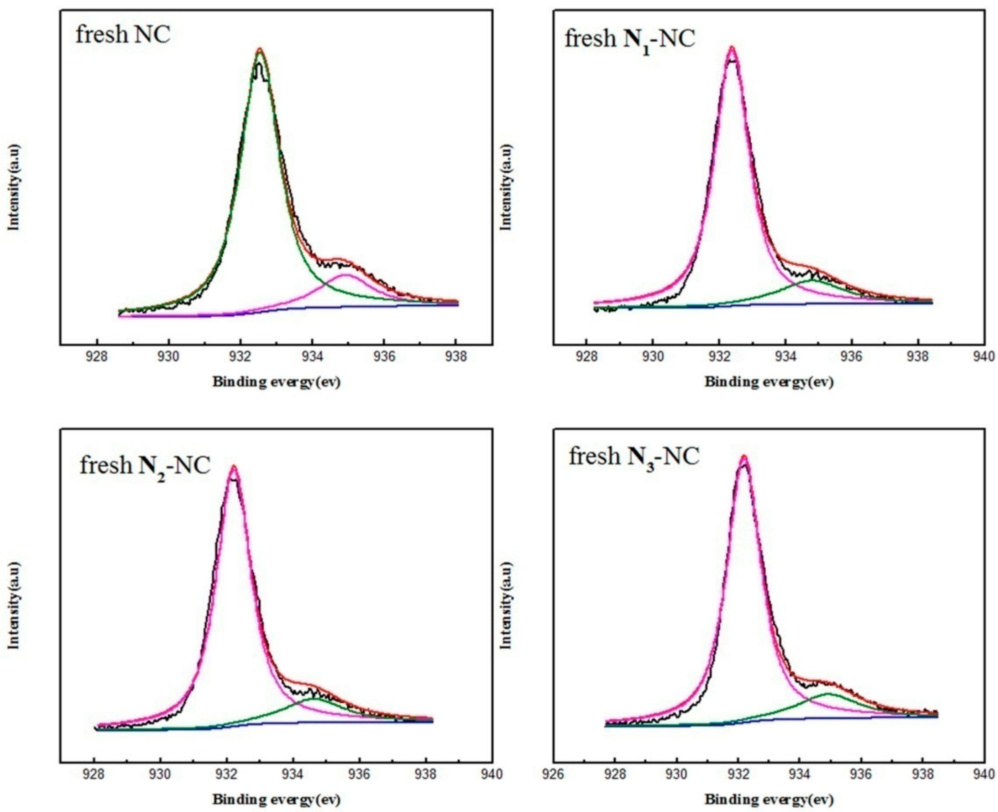

Figure 9. *Cont.*

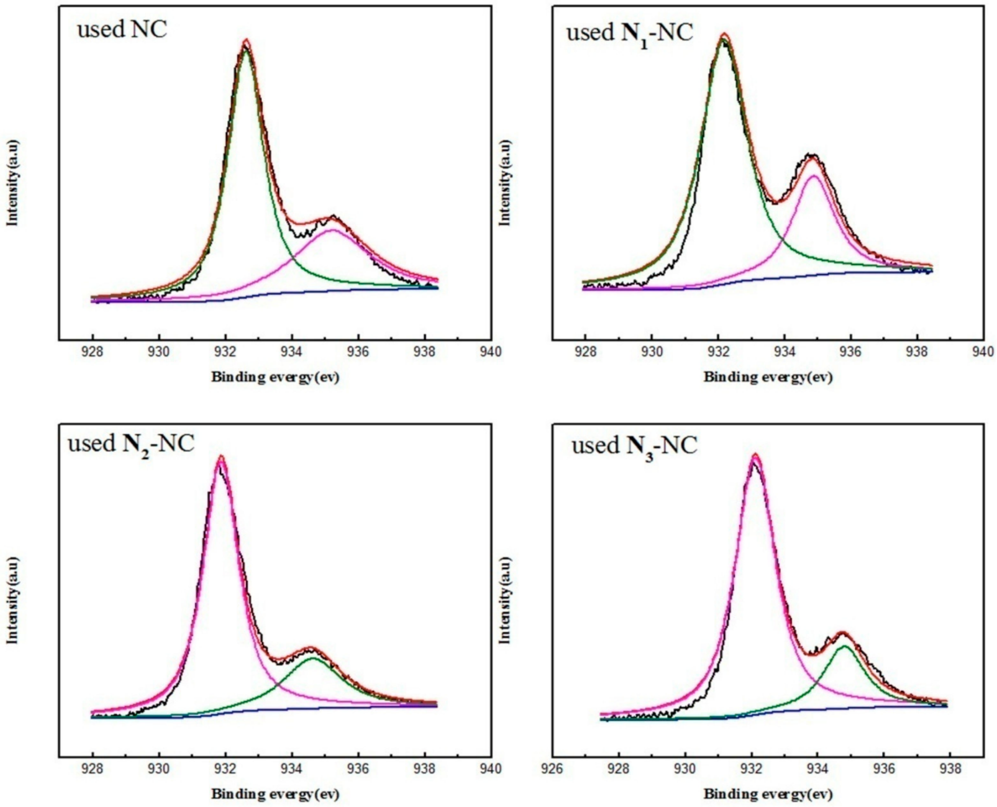

Figure 9. High-resolution XPS spectra of Cu $2p_{3/2}$ of the fresh and used catalysts.

3. Experimental Section

3.1. Materials and Catalyst Preparation

Reagent-grade CuCl (99%), NH_4Cl (purity $\geq$ 99.5%), nitrilotriacetic acid (**N_1**), *N*-(2-hydroxyethyl)iminodiacetic acid (**N_2**), *N*-(2-acetamido)iminodiacetic acid (**N_3**) were purchased from Energy Chemical.

The Nieuwland catalyst's (NC) existing **N_1**, **N_2** and **N_3** are denoted as **N_1**-NC, **N_2**-NC and **N_3**-NC respectively. The amounts of **N_1–N_3** were 4.5 mol % based on cuprous chloride (1.28 g, 1.19 g and 1.28 g, respectively). The structures of the three ligands are shown in Figure 10.

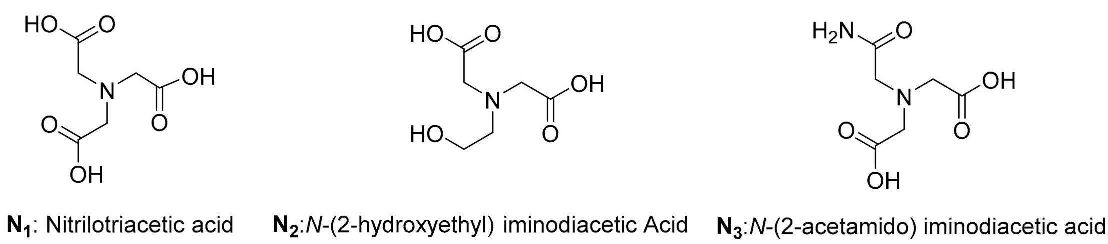

Figure 10. The structure of the three ligands.

3.2. The Dimerization Reaction of C_2H_2

A schematic diagram of the C_2H_2 dimerization system is shown in Figure 11. The reaction was carried out in a self-designed bubble-bed reactor with a length of 400 mm, an external diameter of 40 mm, and an inside diameter 20 mm. Before the start of the reaction, the reactor was purged with nitrogen to remove air, then 8 g (0.15 mol) of NH_4Cl was dissolved in 15 mL of deionized water to obtain a solution at 80 °C, which was poured into the bubbled bed reactor. Subsequently, 14.81 g (0.15 mol) of CuCl and $\mathbf{N_1}$–$\mathbf{N_3}$ were added to this solution. Finally, this reactor was purged with nitrogen for 15 min until these solids were dissolved completely to obtain the desired catalyst solutions at 80 °C. The purified C_2H_2 was then transferred into the reactor. The gas phase products (Scheme 2) were analyzed online by a Gas Chromatograph (GC-2014C) equipped with a flame ionization detector.

$$\mathrm{HC{\equiv}CH} + \mathrm{HC{\equiv}CH} \longrightarrow \mathrm{HC{\equiv}C{-}CH{=}CH_2}\ \text{(MVA)}$$
$$\mathrm{HC{\equiv}CH} + \mathrm{H_2O} \longrightarrow \mathrm{CH_3CHO}$$
$$\mathrm{HC{\equiv}C{-}CH{=}CH_2} + \mathrm{HC{\equiv}CH} \longrightarrow \mathrm{H_2C{=}HC{-}C{\equiv}C{-}CH{=}CH_2}\ \text{(DVA)}$$
$$\mathrm{HC{\equiv}C{-}CH{=}CH_2} + \mathrm{HCl} \longrightarrow \mathrm{H_2C{=}\underset{\displaystyle Cl}{\underset{|}{C}}{-}CH{=}CH_2}\ \text{(CP)}$$

Scheme 2. The gas phase products of C_2H_2 dimerization.

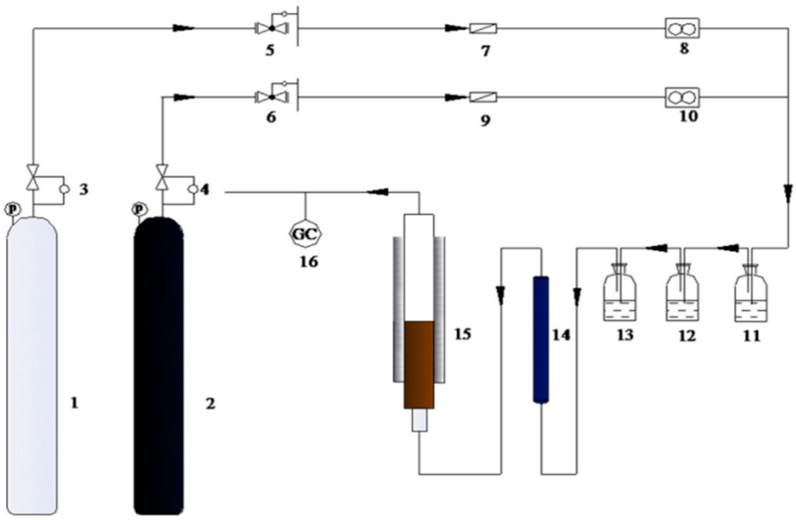

Figure 11. Schematic diagram of the C_2H_2 dimerization system: 1 C_2H_2; 2 N_2; 3,4 partial pressure valve; 5,6 check valve; 7,9 gas filter; 8,10 mass flow controller; 11 $K_2Cr_2O_7$ solution; 12 $Na_2S_2O_4$ solution; 13 NaOH solution; 14 drying tube; 15 reactor; 16 Gas Chromatograph (GC-2014C).

3.3. Catalyst Performance Evaluation

The transformation of C_2H_2 (X) and the selectivity of MVA (S) are respectively defined as the standards for catalytic performance:

$$X\% = [(\beta 2 + 2\beta 3 + 2\beta 4 + 3\beta 5)/(\beta 1 + \beta 2 + 2\beta_3 + 2\beta_4 + 3\beta_5)] \times 100\% \quad (1)$$

$$S\% = [2\beta_3/(\beta_2 + 2\beta_3 + 2\beta_4 + 3\beta_5)] \times 100\% \quad (2)$$

where β_1, β_2, β_3, β_4, and β_5 are the volume fractions of C_2H_2; CH_3CHO; MVA; 2-chloro-1,3-butadiene; and 1,5-hexadien-3-yne (DVA) in the gas products.

3.4. Separation of Crystal from the Catalyst Solution

The crystal A was obtained by means of cooling and crystallization of the Nieuwland catalyst solution (NC) at 3 °C. The crystal A was then washed and filtrated from the catalyst solution and dried in a 55 °C vacuum oven to obtain a characterization solid catalyst. The $\mathbf{N_1}$-NC, $\mathbf{N_2}$-NC, and $\mathbf{N_3}$-NC were treated via the same method to obtain crystals B, C, and D, respectively.

3.5. Treatment of the Used Catalyst Solutions

After acetylene dimerization, the precipitate in NC, $\mathbf{N_1}$-NC, $\mathbf{N_2}$-NC, and $\mathbf{N_3}$-NC solutions were filtrated separately, and the catalyst solutions were dried at 55 °C in a vacuum oven.

3.6. Catalyst Characterization

The fourier transform infrared spectroscopy (FT-IR) spectra were obtained using the Bruker Vertex70 FT-IR spectrometer (Karlsruhe, Germany) over a wavenumber range of 500–4000 cm^{-1}. Thermogravimetry-differential thermal analysis (TG-DTG) was conducted using the NETZSCH STA 449 F3 Jupiter (Bavaria, Germany) under an N_2 atmosphere. The temperature varied from room temperature to 900 °C at a rate of 10 °C/min. X-ray diffraction (XRD) data were collected using a Bruker D8 advanced X-ray diffractometer (Karlsruhe, Germany) with Cu-Kα irradiation at 40 kV and 40 mA at the wide angles (10°–90° in 2θ). X-ray photoelectron spectroscopy (XPS) data was recorded using a Kratos AXIS Ultra DLD spectrometer (Manchester, UK) with a monochromatized Al-Kα X-ray source. Elemental analysis of crystals was performed with X-ray fluorescence (XRF), using an XRF-1800 system (Rh target) attached with HS Easy software (Tokyo, Japan) at 40 kV and 1 mA. Temperature programmed desorption-mass (TPD-MS) experiments were performed with the Micromeritic ASAP 2720 (Atlanta, GA, USA) equipped with a TCD detector. Ultraviolet-visible spectroscopy (UV-Vis) spectra of the samples were obtained using Hitachi U4100 UV spectrometer (Tokyo, Japan) over a wavenumber range of 200–1000 nm.

4. Conclusions

We investigated the effect of nitrogen carboxylate ligands on the Nieuwland catalyst and demonstrated that the ligands having a strong coordination helped to improve the activity of the Nieuwland catalyst. The Nieuwland catalyst containing *N*-(2-acetamido)iminodiacetic acid can increase the yield of MVA by 17.1% compared to ligandless NC. The ligand not only had a strong coordination ability but also had the ability to stabilize the Cu^{+} content, which was beneficial for the catalytic activity and stability. With this strategy, we are further studying the Nieuwland catalyst in our experiments, and the subsequent work will be reported.

Author Contributions: Data curation, Y.Y., J.L. and J.Z.; Funding acquisition, J.Z. and B.D.; Investigation, Y.Y.; Project administration, J.X., J.Z. and B.D.; Supervision, B.D.; Writing—original draft, Y.Y.; Writing—review and editing, J.L. and J.X.

Acknowledgments: We acknowledge National Natural Science Foundation of China (No. 21463021 and 21776179) for their financial support.

Conflicts of Interest: The authors declare no conflicts of interest.

References

1. Rattanasom, N.; Kueseng, P.; Deeprasertkul, C. Improvement of the mechanical and thermal properties of silica-filled polychloroprene vulcanizates prepared from latex system. *Appl. Polym. Sci.* **2012**, *124*, 2657–2668. [CrossRef]
2. Ismail, H.; Leong, H.C. Curing characteristics and mechanical properties of natural rubber/chloroprene rubber and epoxidized natural rubber/chloroprene rubber blends. *Polym. Test.* **2001**, *20*, 509–516. [CrossRef]
3. Liu, J.G.; Han, M.H.; Zuo, Y.Z.; Wang, Z.W. Research progress of dimerization of C_2H_2 to monovinylacetylene. *Chem. Ind. Eng. Prog. (Huagong Jinzhan)* **2011**, *30*, 942–947. [CrossRef]
4. Nieuwland, J.A.; Vogt, R.R. Catalyst and Process of Employing Same. US Patent 1926055A, 12 September 1930.
5. Nieuwland, J.A.; Calcott, W.S.; Downing, F.B.; Carter, A.S. Acetylene polymers and their derivatives. I. the controlled polymerization of acetylene. *J. Am. Chem. Soc.* **1931**, *53*, 4197–4202. [CrossRef]
6. Trotus, I.T.; Zimmermann, T.; Schuth, F. Catalytic reactions of acetylene: A feedstock for the chemical industry revisited. *Chem. Rev.* **2014**, *114*, 1761–1782. [CrossRef] [PubMed]

7. Liu, J.G.; Zuo, Y.Z.; Han, M.H.; Wang, Z.W.; Wang, D.Z. Stability improvement of the Nieuwland catalyst in the dimerization of acetylene to monovinylacetylene. *J. Nat. Gas. Chem.* **2012**, *21*, 495–500. [CrossRef]
8. Tachiyama, T.; Yoshida, M.; Aoyagia, T.; Fukuzumi, S. Mechanistic study on dimerization of acetylene with a Nieuwland catalyst. *Appl. Organomet. Chem.* **2008**, *22*, 205–210. [CrossRef]
9. Liu, Z.H.; Yu, Y.L.; Tao, C.Y.; Du, J.; Liu, R.L.; Fan, X.; Peng, M.; Sun, D.G.; Zuo, Z.H.; Ma, J.X.; Xie, Z.M.; Li, Z.Q. A Method of Dimerization of C2H2 to Monovinylacetylene. CN Patent 102775266 A, 14 November 2012.
10. Han, M.H.; Liu, J.G.; Zuo, Y.Z.; Wang, Z.W. The Method and Application of Anhydrous Nieuwland Catalyst during Dimerization of C2H2. CN Patent 103285925 A, 11 September 2013.
11. Liu, Z.H.; Yu, Y.L.; Tao, C.Y.; Du, J.; Liu, R.L.; Fan, X.; Peng, M.; Sun, D.G.; Zuo, Z.H.; Ma, J.X. A Method of Synthesizing Monovinylacetylene in Aqueous Solution. CN Patent 102731241 A, 17 October 2012.
12. Liu, Z.H.; Yu, Y.L.; Du, J.; Fan, X.; Tao, C.Y. Acetylene dimerization catalyzed by $LaCl_3$-modified Nieuwland catalyst. *CIESC J.* **2014**, *65*, 1260–1266. [CrossRef]
13. Du, J.; Liu, Z.H.; Tao, C.Y. A Method of Synthesizing Monovinylacetylene. CN Patent 102964198 A, 13 March 2013.
14. Zhang, Y.K.; Jia, Z.K.; Zhen, B.; Han, M.H. Acetylene dimerization catalyzed by Nieuwland catalyst. *CIESC J.* **2016**, *67*, 294–299. [CrossRef]
15. Lu, J.L.; Xie, J.W.; Liu, H.Y.; Liu, P.; Liu, Z.Y.; Dai, B. Strontium chloride modified Nieuwland catalyst in the dimerization of acetylene to monovinylacetylene. *Asian J. Chem.* **2014**, *26*, 8211–8214. [CrossRef]
16. Lu, J.L.; Liu, H.Y.; Xie, J.W.; Liu, P.; Liu, Z.Y.; Dai, B. Study on catalytic activity of zinc(II)-copper(I) collaborative bimetallic catalysis in acetylene dimerization reaction. *J. Shihezi Univ.* **2014**, *32*, 213–217. [CrossRef]
17. Lu, J.L.; Liu, H.Y.; Xie, J.W.; Liu, P.; Dai, B.; Liu, Z.Y. Effect of polyethylene glycol/Nieuwland catalyst on C_2H_2 dimerization reaction. *Chem. Eng.* **2015**, *43*, 60–64. [CrossRef]
18. Liu, J.; Han, M.; Wang, Z. Effect of solvent on catalytic performance of anhydrous catalyst in acetylene dimerization to monovinylacetylene. *J. Energy Chem.* **2013**, *22*, 599–604. [CrossRef]
19. You, Y.H.; Luo, J.; Xie, J.W.; Dai, B. Effect of iminodiacetic acid-modified Nieuwland catalyst on the C_2H_2 dimerization reaction. *Catalysts* **2017**, *7*, 394. [CrossRef]
20. Liu, H.Y.; Xie, J.W.; Liu, P.; Dai, B. Effect of Cu^+/Cu^{2+} Ratio on the Catalytic Behavior of Anhydrous Nieuwland Catalyst during Dimerization of C_2H_2. *Catalysts* **2016**, *6*, 120. [CrossRef]